ACI STRUCTURAL JOURNAL TECHNICAL PAPER

Title No. 116-S69

Effect of Sustained Service Loading on Post-Fire Flexural Response of Reinforced Concrete T-Beams

by Chanachai Thongchom, Akhrawat Lenwari, and Riyad S. Aboutaha

This paper presents the effect of sustained service loading at elevated temperatures on the residual flexural response of reinforced concrete (RC) T-beams after exposed to elevated temperatures of 700 and 900°C (1292 and 1652°F) for 3 hours and then cooled in air. Two beams were subjected to a constant simulated service loading equal to 22.6% of undamaged (unheated) flexural strength, while the counterpart beams were exposed to fire without any applied sustained load. The test results showed that the bottom (tension) steel reinforcements in all fire-exposed beams had experienced the peak temperatures that were higher than a critical value (593°C [1099°F]) before the post-fire static test. The post-fire static test results showed that the sustained loading has a detrimental effect on the post-fire flexural response of RC beams. The effect was more pronounced on the post-fire stiffness and ductility than on strength. In the paper, simplified finite element models for predicting the temperature response and post-fire load-deflection relationships of fire-exposed RC beams are also described.

Keywords: elevated temperatures; finite element analysis; fire damage; flexural response; reinforced concrete beams; sustained service loading; thermal response.

INTRODUCTION

Reinforced concrete (RC) members have been widely recognized for their high fire resistance characteristics. During a fire, the temperature history of steel reinforcements is the most important factor affecting the structural behavior of RC beams.[1] Steel reinforcements might be directly exposed to the effects of elevated temperature if concrete spalling occurred due to combinations of internal water pressure and high thermal stresses.[2] The load-carrying capacity of RC members tends to decrease as the steel temperature increases above 400°C (752°F).[3] Creep of steel reinforcement is obvious when temperature at the reinforcement exceeds 400°C (752°F). Creep of concrete under a constant load and stabilized temperature is influential at temperatures above 400°C (752°F).[4,5] The strength of bond between concrete and steel reinforcement significantly influences the fire resistance of reinforced concrete structures, especially when temperature at the steel reinforcement is higher than 500°C (932°F), and the assumption of perfect bond condition in the analysis of RC structures under fire becomes unconservative.[6] An increasing level of sustained loading on RC beams exposed to fire caused larger deflection, early yielding of steel reinforcement, increased mechanical and creep strains, and reduced fire resistance time.[7]

After fire, the structural performance of RC members can significantly deteriorate due to the unrecoverable loss in mechanical properties of concrete, steel reinforcements, and bonding between steel bars and the surrounding concrete. In a study by Neves et al.,[8] quenched and self-tempered bars (QST bars) experienced more degradation in the residual behavior than carbon-steel bars for exposure temperatures above 550°C (1022°F).[9] Lenwari et al.[10] investigated the compressive strength of standard Ø150 x 300 mm (Ø5.9 x 11.8 in.) concrete cylinders after exposure to 300, 500, and 700°C (572, 932, and 1292°F) for 2 hours (for all temperatures) and 3 hours (only for 700°C [1292°F]). The test results showed that low-strength concrete was more susceptible to the loss in residual properties caused by fire than high-strength concrete.

The safety and serviceability of fire-damaged RC structures are keys to making decisions on future repair or strengthening actions to prolong the service life. Typically, RC members are subjected to some degree of service loading beyond the cracking load during fire incidents. Past experimental studies on the residual flexural response of fire-damaged RC beams simulated the effect of fire using either constant elevated temperature or standard fire exposure. El-Hawary et al.[11] tested RC beams after exposure to fire at a constant elevated temperature of 650°C (1202°F) for 0.5, 1, and 2 hours and cooled by water. No sustained loading was applied during heating and cooling. The test results showed that post-fire flexural strengths were less than the unheated strength by 11.8, 19.3, and 38.7% after exposure for 0.5, 1, and 2 hours, respectively. Hansanti[12] investigated the residual flexural response of rectangular RC beams after exposure to ASTM E119 standard fire for 0.5, 1, and 1.5 hours and cooled in air. No sustained loading was applied during heating and cooling. The test results showed that effects of fire on the post-fire yield and ultimate strengths were minimal for heating periods of 0.5 and 1 hour. For heating period of 1.5 hours, however, the yield and ultimate strengths of fire-damaged beams decreased from the unheated values by 16% and 15%, respectively. Kumar and Kumar[13] investigated the residual strengths of simply supported reinforced cement concrete (RCC) beams after exposure to the ISO 834 standard fire for 1, 1.5, 2, and 2.5 hours. No load was applied during fire exposure. The test results showed that residual strengths decreased by 17% and 50% after exposure for 1 and 2 hours, respectively. Xu et

ACI Structural Journal, V. 116, No. 3, May 2019.

MS No. S-2018-214, doi: 10.14359/51714477, received June 7, 2018, and reviewed under Institute publication policies.

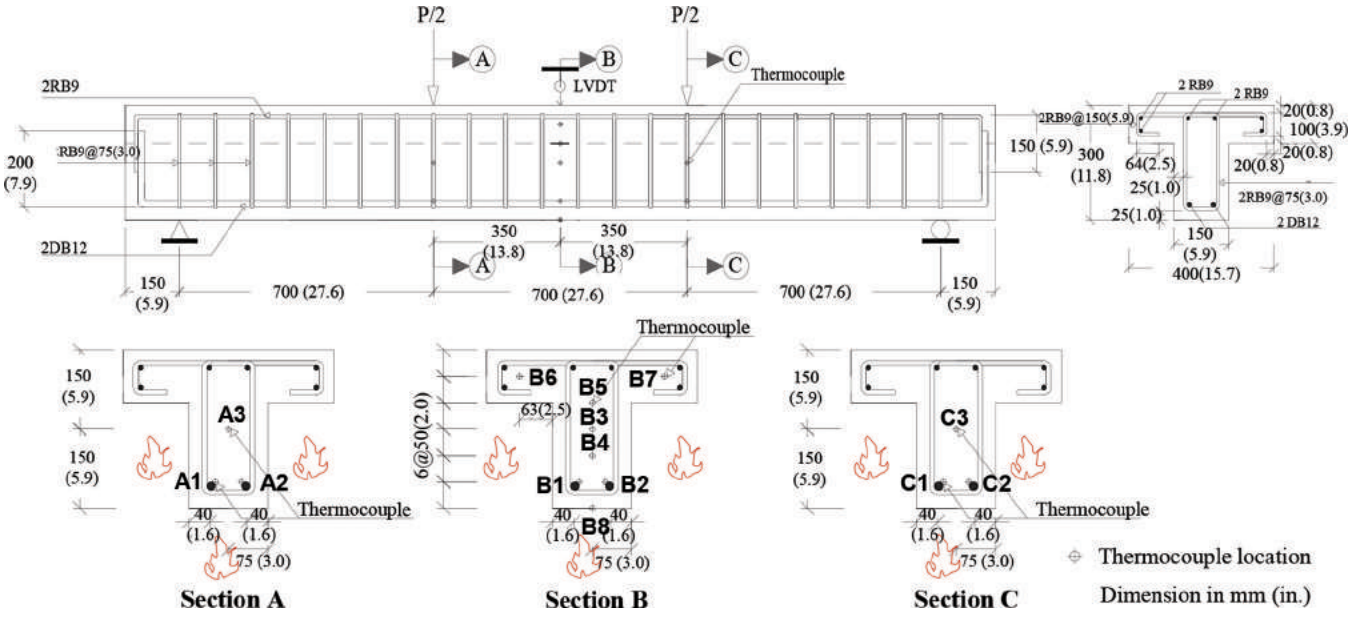

Fig. 1—Static test setup for RC T-beams.

al.[14] investigated the residual flexural behavior of two rectangular RC beams and one RC T-beam after exposure to the ISO 834 standard fire for 2 hours without sustained loading. The test results showed that the assumption of plane section was applicable for RC T-beams. Also, the flexural capacity of rectangular beams decreased by 18.5% after fire exposure.

Past analytical studies on the post-fire response of RC structures can be classified into two methods, namely the section analysis method and the finite element (FE) method. Lakhani et al.[15] assessed the post-fire load-deflection of RC beams using the lumped system concept. A beam cross section was divided into a number of sectors. A finite difference method was used in the thermal analysis to estimate the peak temperature distribution within the cross section. Then, the moment-curvature relationships were constructed using residual mechanical properties of concrete and steel in each sector based on the calculated peak temperature. These moment-curvature relationships were used to define zero length springs in the nonlinear static pushover analysis to obtain the load-deflection relationships. Ožbolt et al.[16] employed a transient thermo-mechanical model to investigate the coupled thermal-mechanical behavior of RC members. The temperature-dependent microplane model was used as a constitutive law for concrete. A three-dimensional (3-D) FE model was developed within the framework of continuum mechanics and irreversible thermodynamics. Kodur and Agrawal[17,18] proposed a nonlinear FE analysis using ABAQUS that incorporated distinct material properties of steel reinforcement and concrete during fire exposure (both heating and cooling phases) and residual (after cooling) phase. The analysis results showed that large irrecoverable plastic deformations could remain in fire-exposed RC beams. Large residual deformations led to the lower post-fire residual capacity. From the parametric study, the sustained loading present during the fire exposure significantly influences both post-fire residual capacity and deformation of RC beams.

Based on the literature review, previous studies that emphasized the effect of sustained loading on the post-fire flexural response of RC beams have been limited in the literature. The main objectives of this research are as follows: 1) to investigate the effects of sustained service loading during fire exposure on thermal and creep deflection responses of simply supported RC T-beams subjected to elevated temperatures of 700 and 900°C (1292 and 1652°F) for 3 hours; 2) to investigate the effects of sustained service loading on post-fire flexural response of RC beams after cooling; and 3) to propose a simplified analysis for predicting the post-fire flexural response of RC beams.

RESEARCH SIGNIFICANCE

The presence of sustained service loads at elevated temperatures deteriorates the post-fire performance of RC structures. Most previous studies have emphasized on rectangular RC beams with no sustained loading during fire exposure. This research shows that sustained loading promoted creep deflection at elevated temperatures and had a detrimental effect on the post-fire flexural response of RC beams. The effect was more pronounced on the post-fire stiffness and ductility than strength.

EXPERIMENTAL PROGRAM

Tested beams

A total of five simply supported RC T-beams of identical section were tested under static four-point bending as shown in Fig. 1. The T-section has an overall depth of 300 mm (11.8 in.), web thickness of 150 mm (5.9 in.), flange width of 400 mm (15.7 in.), and flange thickness of 100 mm (3.9 in.). The span length was 2100 mm (82.7 in.). Two DB12 (0.5 in.) were used as the bottom (tension) reinforcements in the web, while six RB9 (0.4 in.) were used as the longitudinal reinforcements in the flange. Transverse reinforcements (RB9 [0.4 in.]) in the flange had a constant spacing of 150 mm (5.9 in.). Web-shear stirrups (RB9 [0.4 in.]) had a constant spacing of 75 mm (3.0 in.). The concrete cover thicknesses

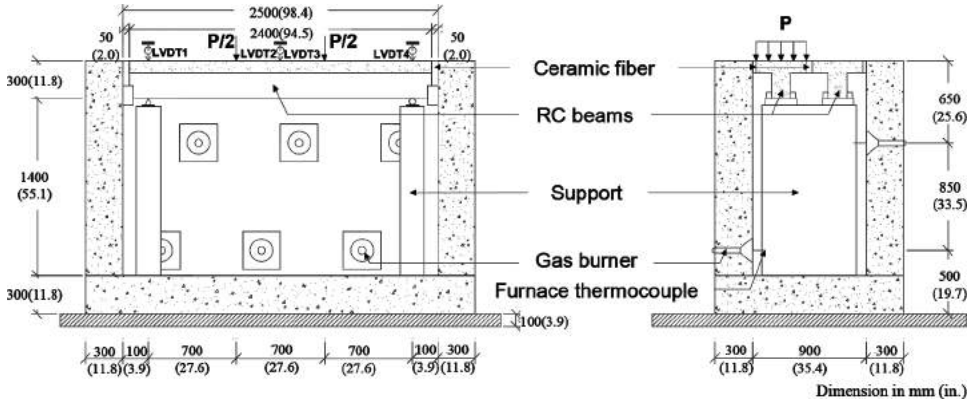

Fig. 2—Test setup for pair of RC T-beams inside fire test furnace.

over DB12 (0.5 in.) and RB9 (0.4 in.) reinforcements were 25 (1.0) and 20 (0.8) mm (in.), respectively. Based on the concrete covering thickness, the tested beams were deemed to satisfy the fire resistance rating of two hours under a standard building fire in accordance with the International Building Code (ICC 2015).[19]

All beams and standard Ø150 x 300 mm (Ø5.9 x 11.8 in.) concrete cylinders were cast from the same batch. After 24 hours, the beams and cylinders were demolded and cured with plastic sheeting at the ambient temperature (approximately 35°C [95°F]) for 28 days. After curing, a control beam (CB) was static tested at the ambient temperature to provide the undamaged (unheated) flexural response including the load-deflection relationship (stiffness, strength, and ductility), crack pattern, and failure mode. Strain gauges were installed at the bottom and top steel reinforcements. In the static test, the beam was periodically unloaded and reloaded until failure. Initially, a load increment between consecutive unloading points was 20 kN (4.5 kip). After yielding of the beam, a displacement increment between unloading points was controlled at approximately 2 mm (0.08 in.). Four other beams were fire-damaged before the static test. Heating and cooling of these beams will be described in the following section.

Heating and cooling

Figure 2 shows the test setup for heating four RC beams inside the fire test furnace. Internal dimensions of the furnace were 900 x 2500 x 1700 mm (35 x 98 x 67 in.). The furnace was equipped with six LPG-fueled burners at two levels above the furnace floor. The average furnace temperature was obtained from six thermocouples installed alongside the burners. The web and bottom of flange of beams were exposed to fire, which simulates a fire beneath the floor scenario. Type-K thermocouples were installed to measure the temperatures at concrete and tension steel reinforcements in beam sections at midspan and two loading points as shown in Fig. 1. Three linear variable differential transformers (LVDTs) were installed to measure the deflections at midspan and two supports. At each elevated temperature (700 or 900°C [1292 or 1652°F]), two beams were simultaneously exposed to fire in an unrestrained condition. One beam (B700(S) or B900(S)) was subjected to a constant simulated service loading under four-point bending identical to Fig. 1, while the counterpart beam (B700 or B900) was exposed to fire without any applied sustained load. The simulated service loading at elevated temperatures was 31.6 kN (7.1 kip). The simulated service loading was applied by a hydraulic jack at 15 min before heating and maintained constant during fire exposure. The average time-temperature relationship inside the furnace was initially controlled to follow the ISO 834[20] standard fire curve. Once the target temperature of 700 or 900°C (1292 or 1652°F) was reached, the average temperature was maintained for a heating period of 3 hours. For Beams B700 and B700(S), however, the heating was extended by 30 minutes to compensate the sudden drop of furnace temperature from 700°C (1292°F) caused by a burner control problem. After heating, all beams were left inside the furnace to allow natural air cooling to the ambient temperature. The applied loading was removed when the average steel temperature dropped to below 400°C (752°F). All fire-exposed beams were subsequently tested under static four-point bending to failure using the same procedure to provide the fire-damaged flexural response.

To determine whether a failure of RC beams occurred during exposure to the specified elevated temperature (700 or 900°C [1292 or 1652°F]), two failure criteria were chosen. In the first criterion, the fire resistance time was taken as the time when the temperature of the steel reinforcement reached a critical value of 593°C (1099°F).[21] In the second criterion, the failure was deemed to occur when the deflection reached $L/20$ mm (105 mm [4.1 in.]) or the rate of deflection exceeded $L^2/(9000d)$ mm/min (1.9 mm/min [0.07 in./min]).[22] The rate of deflection was considered when the deflection exceeded $L/30$ (70 mm [2.8 in.]).

Material properties

Concrete—In the study, a ready mixed concrete was used. The concrete consisted of Type I portland cement, river sand (fine aggregate), and natural rock (coarse aggregate). The maximum size of coarse aggregates was 19 mm (0.7 in.). The water-cement ratio was 0.44. The mixture proportion was as follows: cement—366 kg/m^3 (22.8 lb/ft^3); water—160 kg/m^3 (10.0 lb/ft^3); fine aggregate—750 kg/m^3 (46.8 lb/ft^3); and coarse aggregate—1150 kg/m^3 (71.8 lb/ft^3).

To assess the post-fire mechanical properties of concrete, the standard Ø150 x 300 mm (Ø5.9 x 11.8 in.) concrete cylinders were exposed to fire simultaneously with RC beams

Table 1—Compressive strengths of fire-damaged concrete cylinders

Cylinder specimen No.	Specimen age, days		Exposure temperature, °C (°F)	Density, kg/m^3 (lb/ft^3)		Compressive strength from destructive test, MPa (ksi)	
	Heating	Testing		Before heating	After heating	Test value	Mean ± SD*
CRT-1	—	103	Room	2422 (151)	—	42.4 (6.1)	43.0 (6.2) ± 0.6
CRT-2	—	103		2418 (151)	—	43.0 (6.2)	
CRT-3	—	103		2427 (152)	—	43.6 (6.3)	
C700-1	87	103	700 (1292)	2407 (150)	2212 (138)	5.2 (0.8)	6.2 (0.9) ± 1.7
C700-2	87	103		2412 (151)	2267 (142)	5.2 (0.8)	
C700-3	87	103		2442 (152)	2295 (143)	8.2 (1.2)	
C700-4	87	109	700 (1292)	2418 (151)	2238 (140)	6.7 (1.0)	6.6 (1.0) ± 1.5
C700-5	87	109		2423 (151)	2276 (142)	5.0 (0.7)	
C700-6	87	109		2389 (149)	2232 (139)	8.0 (1.2)	
C900-1	189	231	900 (1652)	2346 (146)	N/A†	3.1 (0.4)	2.6 (0.4) ± 0.8
C900-2	189	231		2404 (150)	N/A†	1.6 (0.2)	
C900-3	189	231		2407 (150)	N/A†	3.0 (0.4)	

*Mean and standard deviation from 10 readings.

†No data was obtained.

at each elevated temperature. All cylinders were placed at the bottom of the fire test furnace. Table 1 summarizes the density and compressive strength values of fire-damaged concrete cylinders. The specimen ages at the time of heating and testing are also given. From the destructive compression test, an average compressive strength of unheated concrete cylinders was 43.0 MPa (6.2 ksi). Mean residual compressive strengths of cylinders exposed to 700 and 900°C (1292 and 1652°F) were 6.4 and 2.6 MPa (0.9 and 0.4 ksi), respectively.

Steel reinforcements—Two sizes of steel reinforcement were used. The measured elastic modulus, yield strength, and ultimate strength of 12 mm (0.5 in.) diameter deformed bars (DB12 [0.5 in.]) were 200,417, 532, and 640 MPa (29,068, 77, and 93 ksi), respectively. The measured elastic modulus, yield strength, and ultimate strength of 9 mm (0.4 in.) diameter round bars (RB9 [0.4 in.]) were 194,700, 346 and 550 MPa (28,239, 50, and 80 ksi), respectively.

EXPERIMENTAL RESULTS AND DISCUSSION

Thermal response during heating and cooling

Figures 3 and 4 show the measured thermal response—that is, the temperature histories at concrete and steel reinforcements—of RC beams exposed to 700 and 900°C (1292 and 1652°F), respectively. The measured peak temperatures at the bottom (critical) steel reinforcements in Beams B700, B700(S), B900, and B900(S) were 606, 611, 646, and 659°C (1123, 1132, 1195, and 1218°F), respectively. It was observed that the temperatures continued to rise after heating—that is, the peak temperatures at concrete and steel reinforcements were attained during cooling of furnace. The peak temperature at each location occurred at a different time. Also, the peak steel temperature increased as the exposure temperature increased. The sustained service loading did not significantly influence the peak steel temperature. The bottom steel reinforcements in all fire-damaged beams experienced the peak temperatures above a critical value of 593°C (1099°F) before the post-fire static test. Based on the steel temperature criterion, Beams B900 and B900(S) failed before 3 hours. In summary, the fire resistance times based on the critical temperature criterion of Beams B700, B700(S), B900, and B900(S) were 194, 199, 130, and 135 minutes, respectively. The fire resistance times reported herein are expected to be higher than ones based on the standard test method[20,21] because the constant exposure temperatures (maximum at 900°C [1652°F]) were less than the standard fire ones. The sustained service loading did not significantly influence the fire resistance of RC beams. For the fire beneath the floor scenario where the web and bottom of flange of T-beams were exposed to fire, the temperatures of concrete in the beam flange (Thermocouples No. B5, B6, and B7) were lower than those in the web (Thermocouples No. B3 and B4). Also note that the temperature histories at the concrete surface (Thermocouple No. B8) were similar to the average furnace temperature.

Creep deflection during heating

At the elevated temperatures, the beam deflection increased during fire exposure. Such increase involved creep, drying shrinkage, and cracking of concrete; creep of steel; and deterioration of bonding. A reduction in bond strength between steel reinforcements and surrounding concrete under high temperatures is mainly caused by the difference in the coefficients of thermal expansion of the two materials.[23] The creep strain of steel is caused by the movement of dislocations in the slip plane at high temperature.[24] The test results showed that beams subjected to the simulated service loading in addition to the beam self-weight experienced larger creep midspan deflections at the elevated temperatures. Deformations due to the transient creep were triggered by bottom (tension) steel reinforcements. However, none of beams failed before 3 hours based on the deflection criterion. Figure 5 compares

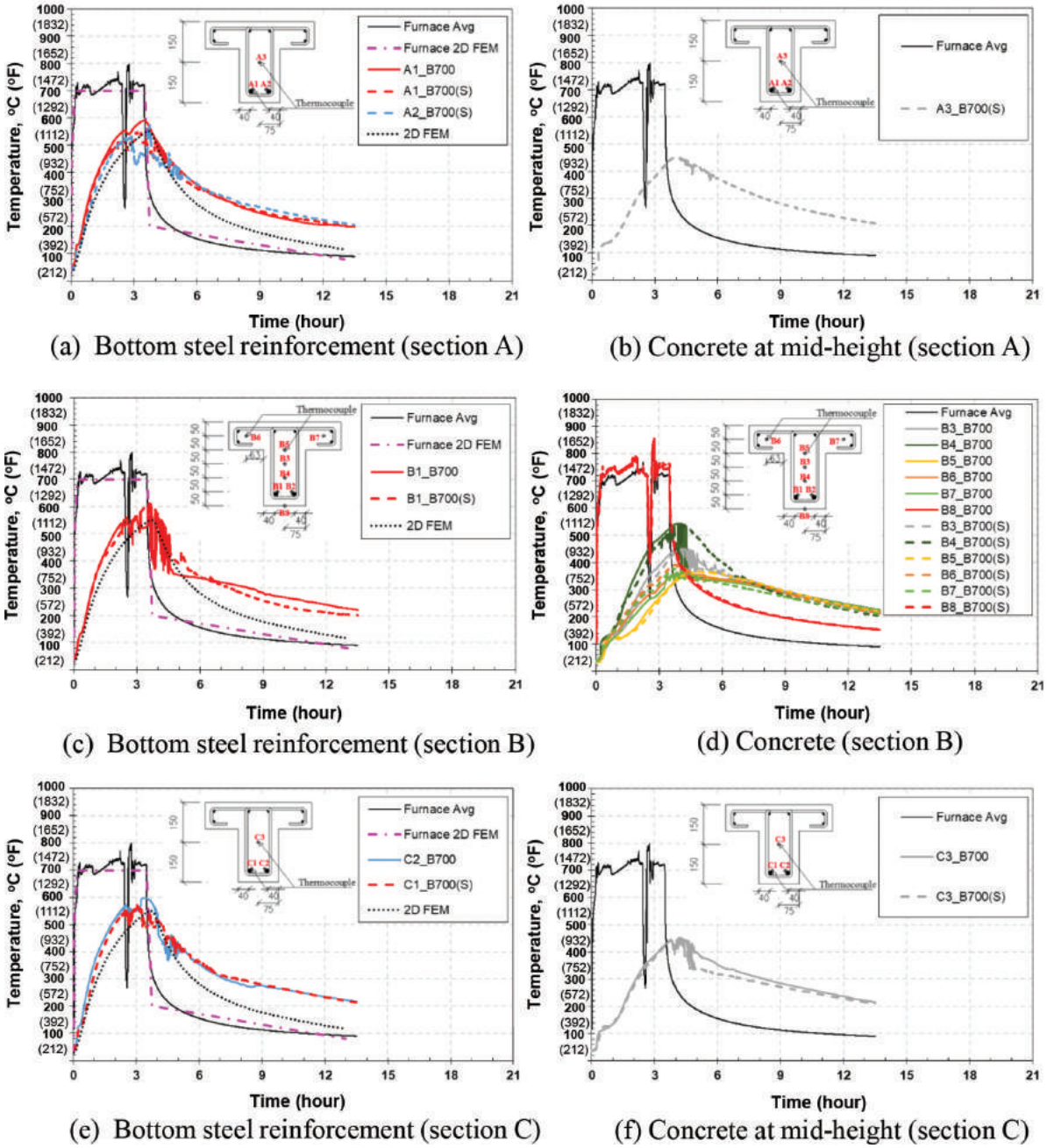

Fig. 3—Measured versus predicted thermal response of Beams B700 and B700(S).

the midspan deflections measured relative to supports—that is, the difference between LVDT No. 2 (or 3) data and the average of LVDTs No. 1 and 4 data—of Beams B900 and B900(S) during heating. The average temperatures of two bottom steel reinforcements (Ts) at different heating times are also indicated in the figure. It was observed that the rate of creep deflection of beam B900(S) subjected to the simulated service loading increased significantly once the steel temperature had exceeded 500°C (932°F). All measured concrete temperatures in the flange were less than 250°C (482°F) when the change in rate of deflection occurred. At the end of heating (3 hours), the midspan deflections of Beams B900 and B900(S) were 15.9 and 46.1 mm (0.6 and 1.8 in.), respectively.

Post-fire flexural response of RC beams

Figure 6 shows visible damage of RC beams after fire exposure. Upon cooling, some recovery of displacement was observed. More damage—that is, cracking, permanent deflection, and concrete spalling—was observed in the beam exposed to higher temperature and subjected to the sustained service loading during fire exposure.

Figure 7 shows the measured load-midspan deflection relationships of beam CB (unheated). The failure of beam CB was caused by yielding of bottom steel reinforcements followed by crushing of concrete, which is typical for beam having an under-reinforced section. The measured cracking, yield, and ultimate loads were 27.0, 99.4, and 140.0 kN (6.1, 22.3, 31.5 kip), respectively. The applied service loading at elevated temperatures was 31.6 kN (7.1 kip). Therefore,

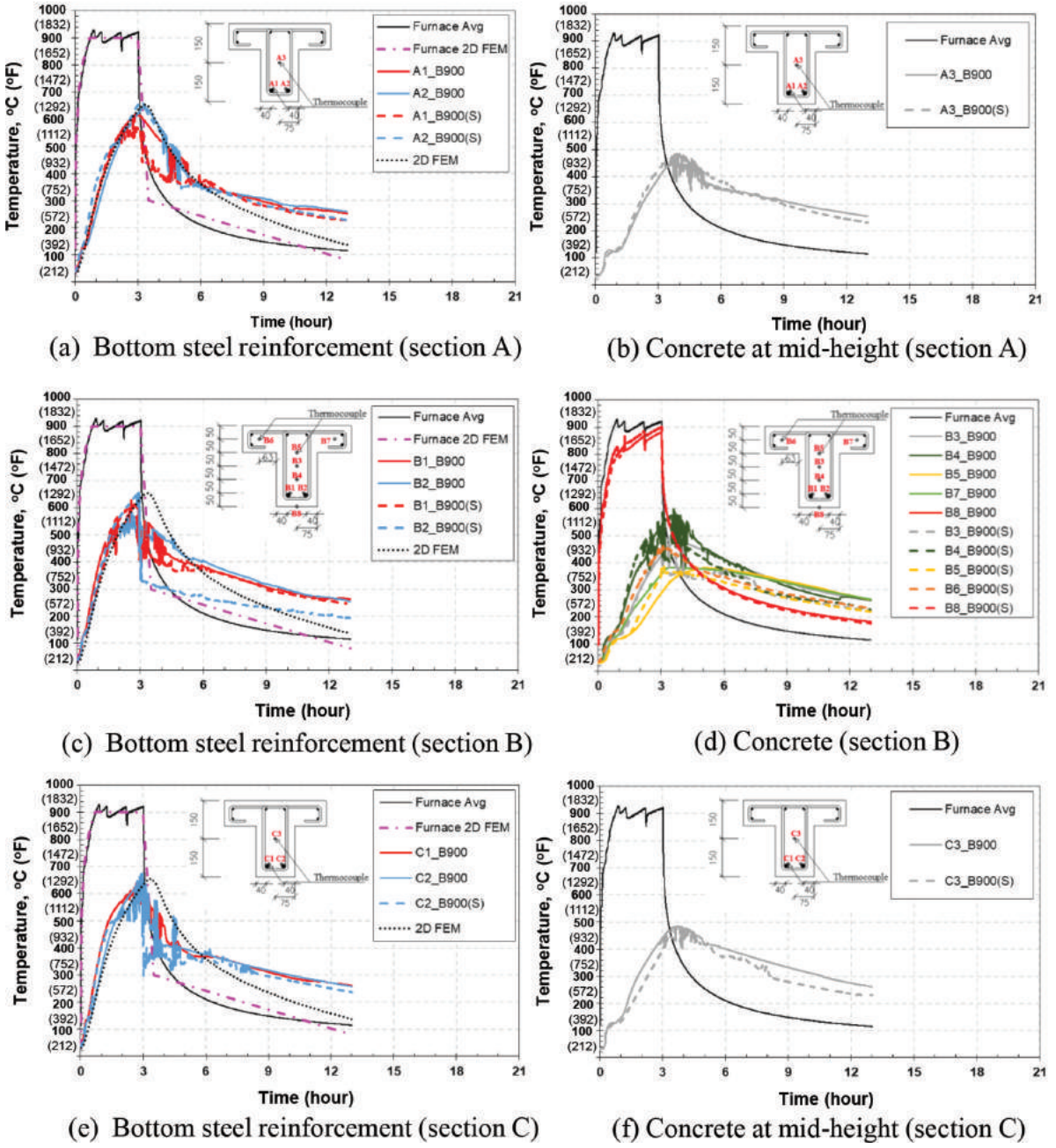

Fig. 4—Measured versus predicted thermal response of Beams B900 and B900(S).

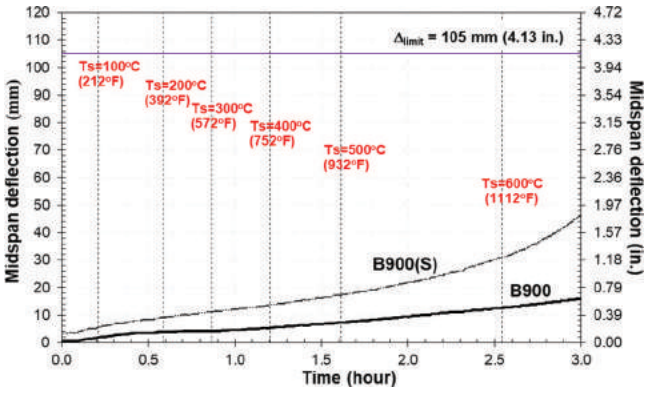

Fig. 5—Midspan deflections of Beams B900 and B900(S) during heating.

this load level corresponded to 22.6% of the unheated load-carrying capacity (140.0 kN [31.5 kip]) and higher than the unheated cracking load (27.0 kN [6.1 kip]). At this load level, the tensile stress at bottom steel reinforcements was approximately 13% of the yield strength of DB12 (0.5 in.) steel.

Figure 7 also shows the measured load-midspan deflection relationships of fire-damaged Beams B700, B700(S), B900, and B900(S). In contrast to Beam CB, there was no obvious cracking load in all fire-damaged beams due to the presence of pre-existing cracks from fire damage. Fig. 8 shows the failure and crack patterns of all tested beams. Concrete crushing was observed in all beams.

Table 2 summarizes the flexural response including the stiffness, yield load, maximum load, ductility index, and failure mode of undamaged and fire-damaged RC beams.

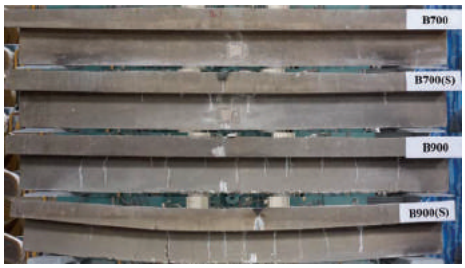

Fig. 6—Visible damage of RC T-beams after exposure to fire.

The ductility index was defined as the ratio between the midspan deflection at the maximum load and one at yield load. The test results showed that the elevated temperatures and sustained service loading reduced the residual flexural response—that is, stiffness and strength, of fire-damaged RC beams. Obviously, the sustained loading has a detrimental effect on the post-fire flexural response of RC beams. The effect was more pronounced on the post-fire stiffness and

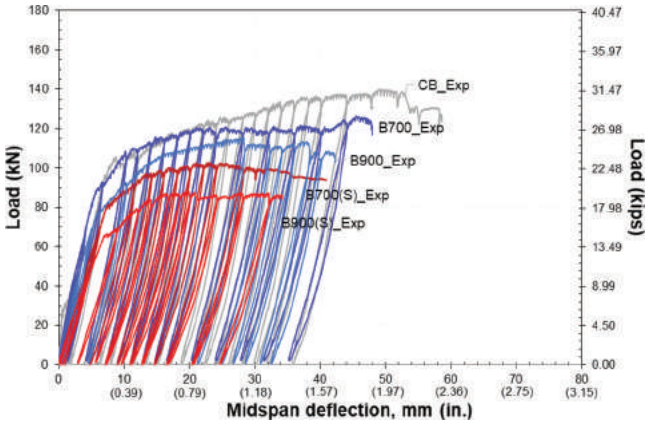

Fig. 7—Load-midspan deflection relationships of control beam and fire-damaged beams.

ductility than strength.

Without the sustained loading (Beam B700), the residual stiffness, yield load, and maximum load were 32, 89, and 90% of the undamaged properties, respectively. With the presence of sustained loading during fire exposure (B700(S)), the residual stiffness, yield load, and maximum load were 20, 80, and 73% of the undamaged properties, respectively. A comparison between Beams B700 and B700(S) showed that the sustained loading decreased the residual stiffness, maximum load, and ductility index by 37, 19, and 64%, respectively.

Without the sustained loading (Beam B900), the residual stiffness, yield load, and maximum load were 25, 72, and 83% of the undamaged properties, respectively. With the presence of sustained loading during fire exposure (beam B900(S)), the residual stiffness, yield load, and maximum load were 16, 65, and 63% of the undamaged properties, respectively. A comparison between Beams B900 and B900(S) showed that the sustained loading decreased the residual stiffness, maximum load, and ductility index by 33, 24, and 45%, respectively.

ANALYTICAL METHODS

2-D transient heat transfer analysis

According to the principle of heat transfer, the heat is transferred from hot gases (thermal loading) to the surface of RC beams by radiation and convection, and then from the surface to interior by conduction. A simplified 2-D transient thermal analysis was performed to investigate the peak thermal response—that is, concrete and steel temperatures—in RC beams. A commercial finite element software[25] was employed. An analysis procedure was extended from the previous work.[26] The beam section was meshed into 2880 elements, as shown in Fig. 9(a). The steel reinforcements were not included in the FE model based on the assumption that they did not significantly influence the temperature distribution in the beam section.[27,28] The temperature at the steel reinforcement was assumed to be the same as the concrete temperature at the position of the steel reinforcement. Concrete was modeled with PLANE55 element. The element had four nodes with one degree of freedom—that is, temperature—at each node. It was applicable to a 2-D steady-state or transient thermal analysis. Carbonate aggregate concrete was assumed. The thermal properties of concrete including the specific heat, density, and thermal conductivity (lower limit) were those specified in the Eurocode 2.[28] Three different moisture contents in concrete of 0, 1.5, and 3% were assumed. An average furnace temperature was applied as convection on lines (section sides) with convection film coefficient values of 25 and 9 W/m^2.K for the exposed and unexposed surfaces, respectively.[17,18,28,29] The exposed surfaces include web and bottom of the flange, while the unexposed surface was top of the flange. For the radiation boundary condition, the emissivity factor was taken as 0.7 from Eurocode 2.[28] A total of 780 thermal load steps were used for the entire heating and cooling of 13 hours.

3-D nonlinear structural analysis

A simplified 3-D nonlinear structural analysis was performed to investigate the post-fire flexural response of RC beams. The following assumptions were made: 1) no slip between concrete and steel reinforcements[14,30]; 2) no concrete spalling[30]; 3) no reduction of concrete compressive strength after fire exposure[31]; 4) no contribution of concrete tensile strength in fire-damaged beams; and 5) the post-fire tensile strength of steel reinforcements depends on the peak steel temperatures experienced during fire exposure. Due to symmetry, a quarter of beam was modeled, as shown in Fig. 9(b). A total of 8620 elements were used. The loading was applied at top of the top steel plate, while the bottom steel plate at the support was restrained in the vertical direction. Concrete was modeled with the SOLID65 element having eight nodes with three degrees of freedom at each node (that is, translations in x, y, and z directions). The element was capable of the plastic deformation, cracking and crushing.

Figure 10(a) shows the modified Hognestad stress-strain model used for concrete. The compressive stress was assumed to be constant after concrete strain reached ε_o which denotes the concrete strain at the maximum compressive stress f_c'. Input values of f_c' and E_c (elastic modulus of concrete: $E_c = 4700\sqrt{f_c'}$) were 43 and 30,820 MPa (6.2 and 4470 ksi),

Table 2—Post-fire static test results of RC T-beams

Beam No. (1)	Beam age, days: Heating (2)	Beam age, days: Static test (3)	Stiffness, kN/m (kip/ft) (4)	Yield load, kN (kip) (5)	Max. load, kN (kip) (6)	Deflection at yield load, mm (in.) (7)	Deflection at max. load, mm (in.) (8)	Ductility index Col.(8)/ Col.(7) (9)	ACI Predicted max. load, kN, (kip) (10)	FEM Predicted max. load, kN, (kip) (11)	ACI test Col.(10)/ Col.(6) (12)	FEM test Col. (11)/ Col.(6) (13)
CB (unheat)	—	128	64,247 (4402)	99.4 (22.3)	140.0 (31.5)	7.6 (0.3)	49.0 (1.9)	6.5	114.4 (25.7)	127.9 (28.8)	0.82	0.91
B700	66	126	20,767 (1423)	88.4 (19.9)	126.5 (28.4)	5.7 (0.2)	45.5 (1.8)	8.0	108.8 (24.5)	110.2 (24.8)	0.86	0.87
B700(S)	66	125	13,057 (895)	79.2 (17.8)	102.7 (23.1)	7.2 (0.3)	21.0 (0.8)	2.9				
B900	189	237	15,742 (1079)	71.5 (16.1)	115.5 (26.0)	5.3 (0.2)	28.3 (1.1)	5.3	106.7 (24.0)	108.2 (24.3)	0.92	0.94
B900(S)	189	237	10,506 (720)	64.4 (14.5)	88.4 (19.9)	6.8 (0.3)	19.5 (0.8)	2.9				

Fig. 8—Failure and crack patterns of RC T-beams.

respectively. For beam CB, the contribution of concrete tensile strength was also considered. The input value of f_r (modulus of rupture: $f_r = 0.62\sqrt{f_c'}$) was 4.1 MPa (0.6 ksi). Due to the presence of pre-existing cracks from fire damage, the resistance of concrete in tension can be ignored for fire-damage beams. Therefore, a zero value of f_r was input for all fire-damaged beams. The Poisson's ratio was assumed to be 0.2. The shear transfer coefficients for open and closed cracks were assumed to be 0.5 and 1.0, respectively. Default values in the software for biaxial crushing stress, hydrostatic stress, biaxial crushing stress, uniaxial crushing stress, and tensile cracked coefficient were used. The steel plate was modeled with the SOLID45 element having eight nodes with three degrees of freedom at each node (that is, translations in x, y, and z directions). The elastic modulus and Poisson's ratio of steel were assumed to be 200 GPa (29,008 ksi) and 0.3, respectively. The steel reinforcements were modeled with the LINK180 element which was a uniaxial tension and compression element having two nodes with three degrees of freedom at each node (that is, translations in x, y, and z directions).

The post-fire stress-stain relationship and mechanical properties of steel reinforcement are assumed to be dependent on the peak steel temperature obtained from the 2-D FEM transient heat transfer analysis. According to Tao et al.,[32] the effect of preloading—that is, the steel being stressed during heating and cooling—tends to increase yield strength and decrease ductility of steel. However, the influence of preloading on the ultimate strength is not significant. Figure 10(b) shows the stress-strain model by Tao et al.[32] used for steel reinforcements as follows.

$$f_{sT} = \begin{cases} E_{sT}\varepsilon_s & 0 \le \varepsilon_s < \varepsilon_{yT} \\ f_{yT} & \varepsilon_{yT} \le \varepsilon_s < \varepsilon_{pT} \\ f_{uT} - (f_{uT} - f_{yT}) \times \left(\dfrac{\varepsilon_{uT} - \varepsilon_s}{\varepsilon_{uT} - \varepsilon_{pT}} \right)^p & \varepsilon_{pT} \le \varepsilon_s < \varepsilon_{uT} \\ f_{uT} & \varepsilon_s \ge \varepsilon_{uT} \end{cases} \quad (1)$$

where f_{sT} and ε_s are the stress and strain of steel reinforcement, respectively. The residual yield strength (f_{yT}) and ultimate strength (f_{uT}) are functions of temperature as

$$f_{yT} = \begin{cases} f_y & T \le 500°\text{C} \\ \left[1 - 5.82 \times 10^{-4}(T - 500)\right] f_y & T > 500°\text{C} \end{cases} \quad (2)$$

$$f_{uT} = \begin{cases} f_u & T \le 500°\text{C} \\ \left[1 - 4.85 \times 10^{-4}(T - 500)\right] f_u & T > 500°\text{C} \end{cases} \quad (3)$$

The value of strain hardening exponent (p) is

$$p = E_{pT} \times \left(\frac{\varepsilon_{uT} - \varepsilon_{pT}}{f_{uT} - f_{yT}} \right) \quad (4)$$

The elastic modulus (E_{sT}) and modulus of elasticity at the onset of strain hardening (E_{pT}) are

$$E_{sT} = \begin{cases} E_s & T \le 500°\text{C} \\ \left[1 - 1.30 \times 10^{-4}(T - 500)\right] E_s & T > 500°\text{C} \end{cases} \quad (5)$$

$$E_{pT} = 0.03 E_{sT} \quad (6)$$

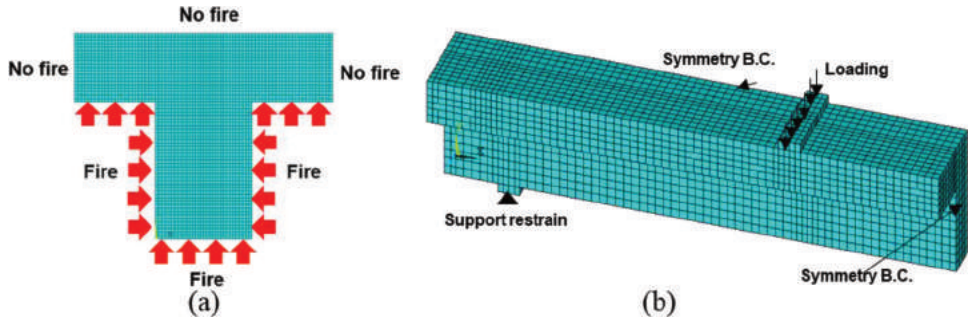

Fig. 9—FE models: (a) 2-D FE model for transient heat transfer analysis; and (b) 3-D FE model for nonlinear structural analysis.

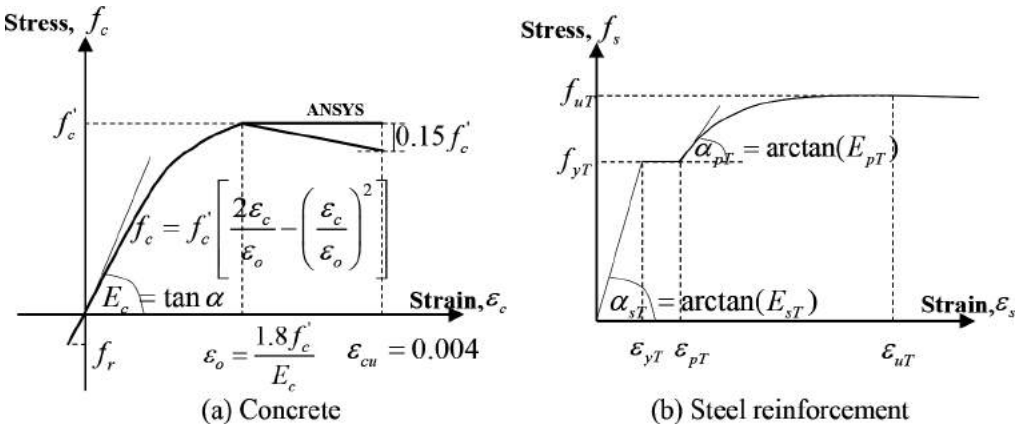

Fig. 10—Stress-strain models for concrete and steel.

The yield strain (ε_{yT}), strain at the onset of strain hardening (ε_{pT}), and ultimate strain corresponding to the ultimate strength (ε_{uT}) are

$$\varepsilon_{yT} = f_{yT}/E_{sT} \tag{7}$$

$$\varepsilon_{pT} = \begin{cases} 15\varepsilon_{yT} & f_y \le 300\,\text{MPa} \\ \left[15 - 0.018(f_y - 300)\right]\varepsilon_{yT} & 300 > f_y \le 800\,\text{MPa} \end{cases} \tag{8}$$

$$\varepsilon_{uT} = \begin{cases} 100\varepsilon_{yT} & f_y \le 300\,\text{MPa} \\ \left[100 - 0.15(f_y - 300)\right]\varepsilon_{yT} & 300 > f_y \le 800\,\text{MPa} \end{cases} \tag{9}$$

In the nonlinear analysis, a monotonic increasing loading with a load step increment of 1 kN (0.2 kip) was applied. For the convergence criterion, the default values were used.

ACI 318 method

In addition to the 3-D nonlinear structural analysis, the ACI 318[33] section analysis method was adopted for predicting the post-fire flexural strength of RC beam sections. Figure 11 shows the symbols used in the section analysis. Main assumptions were: 1) linear strain distribution throughout the beam depth[14,30]; 2) undamaged concrete in compression[31]; 3) no slip between steel and concrete[30]; 4) no tensile stresses in concrete; and 5) the post-fire tensile strength of steel reinforcements depends on the peak steel temperature experienced during fire exposure. Reduced mechanical properties of steel reinforcements by Tao et al.[32] were adopted. The factor β_1, which relates the depth of an equivalent rectangular compressive stress block (a) to the neutral axis depth (c), was as defined by the ACI 318.[33] In this study, the value of β_1 was equal to 0.74. The location of neutral axis (c) was obtained by solving the below equilibrium equation

$$F_c + F_s'' = F_{sT} + F_s' \tag{10}$$

where F_c, F_{sT}, F_s', and F_s'' denote the internal forces in concrete and steel reinforcements as follows

$$F_c = \begin{cases} 0.85f_c'\beta_1 cb_f & c \le t_f \\ 0.85f_c'\beta_1[b_f t_f + b_w(c - t_f)] & c > t_f \end{cases} \tag{11}$$

$$F_{sT} = \begin{cases} E_{sT}\varepsilon_s A_s & \varepsilon_s < \varepsilon_{yT} \\ f_{yT}A_s & \varepsilon_s \ge \varepsilon_{yT} \end{cases} \tag{12}$$

$$F_s' = \begin{cases} E_s'\varepsilon_s' A_s' & |\varepsilon_s'| < \varepsilon_y' \\ f_y' A_s' & |\varepsilon_s'| \ge \varepsilon_y' \end{cases} \tag{13}$$

$$F_s'' = \begin{cases} E_s''\varepsilon_s'' A_s'' & |\varepsilon_s''| < \varepsilon_y'' \\ f_y'' A_s'' & |\varepsilon_s''| \ge \varepsilon_y'' \end{cases} \tag{14}$$

where ε_{yT}, f_{yT}, and E_{sT} are the reduced yield strain, yield strength, and elastic modulus of the bottom steel reinforcements, respectively; ε_y', f_y', and E_s' are the reduced yield strain, yield strength, and elastic modulus of the steel reinforcements near the flange bottom, respectively; ε_y'', f_y'', and E_s'' are the reduced yield strain, yield strength, and elastic

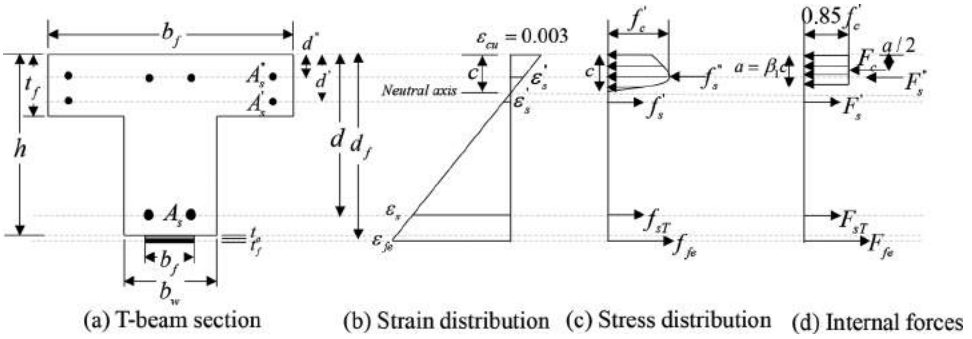

Fig. 11—Section analysis for post-fire flexural strength (refer to ACI 318[33]).

modulus of the steel reinforcements near the flange top, respectively; t_f is the flange thickness; b_w and b_f are the web thickness and flange width, respectively; and A_s, A_s', and A_s'' are the areas of steel reinforcements near the web bottom, flange bottom, and flange top, respectively.

The strains at different steel reinforcement levels (ε_s, ε_s', and ε_s'') are

$$\varepsilon_s = \varepsilon_{cu}\frac{(d-c)}{c} \tag{15}$$

$$\varepsilon_s' = \varepsilon_{cu}\frac{(d'-c)}{c} \tag{16}$$

$$\varepsilon_s'' = \varepsilon_{cu}\frac{(c-d'')}{c} \tag{17}$$

where d, d', and d'' are the distances from an extreme compression fiber to steel reinforcements near the web bottom, flange bottom, and flange top, respectively.

Finally, the nominal post-fire flexural strength (M_n) was calculated from

$$M_n = F_c\left(d-\frac{a}{2}\right)+F_s''(d-d'')-F_s'(d-d') \tag{18}$$

ANALYTICAL RESULTS AND DISCUSSION

Predicted thermal response

In Figures 3 and 4, the 2-D FEM predictions of temperature histories at the bottom (critical) steel reinforcements are also shown for comparison. The predicted peak steel temperatures in Beams B700, B700(S), B900, and B900(S) were 551, 551, 661, and 661°C (1024, 1024, 1192, and 1192°F), respectively. Therefore, the differences between the measured peak steel temperatures and 2-D FEM predictions were less than 10%. Changing the assumed moisture content value in concrete (0, 1.5, and 3%) did not significantly influence the predicted peak steel temperature.

Figures 12(a) and (b) show the 2-D FEM predictions of peak temperature distributions in RC beams exposed to 700 and 900°C (1292 and 1652°F), respectively. Note that the peak temperature at each location occurred at a different time. The 500°C (932°F) isotherm contour is indicated with a dashed line. Obviously, the predicted level of damage—that is peak temperature distribution—was more severe for beams exposed to 900°C (1652°F) than beams exposed to 700°C (1292°F). According to the 500°C (932°F) isotherm method specified in the Eurocode 2[28] for the assessment of RC structures at elevated temperatures, the concrete with a temperature below 500°C (932°F) is assumed to retain its ambient strength. The method is applicable to a reinforced and prestressed concrete with respect to axial load, bending moment and their combinations at elevated temperatures. Based on the method, the damaged concrete with temperature above 500°C (932°F) was mostly in a tension zone below the neutral axis. Concrete in the compression zone was unaffected by fire.

Predicted post-fire load-deflection relationships

Figures 13, 14, and 15 compare the 3-D FEM and ACI predictions with the measured load-midspan deflection relationships of Beams CB, B700 and B700(S), B900 and B900(S), respectively. The maximum loads predicted by 3D FEM and ACI methods are also given in Table 2. A comparison of the test data with predictions showed that both analyses conservatively estimated the residual strengths of beams with no sustained loading effect—that is, CB (unheated), B700, and B900—while they overestimated the residual strengths of beams with sustained loading effect—that is, B700(S) and B900(S). A future work is recommended on appropriate material constitutive models that incorporate the effect of sustained loading during fire exposure.

CONCLUSIONS

In this paper, the effects of sustained service loading at elevated temperatures on the post-fire flexural response of RC T-beams were emphasized. The temperature histories at concrete and steel reinforcements inside RC beams heated at 700 and 900°C (1292 and 1652°F) for 3 hours and air-cooled in the furnace were also investigated. For all fire-exposed beams, bottom (tension) steel reinforcements had experienced the peak temperatures higher than a critical value (593°C [1099°F]) before the post-fire static test. The main conclusions are as follows:

1. The sustained service loading did not significantly influence the peak temperature at critical (bottom) steel reinforcements and fire resistance of RC beams. The fire resistance times based on the critical steel temperature criterion were less than those based on the deflection criterion.

2. The sustained service loading promoted the creep deflection at elevated temperatures. The rate of creep deflection

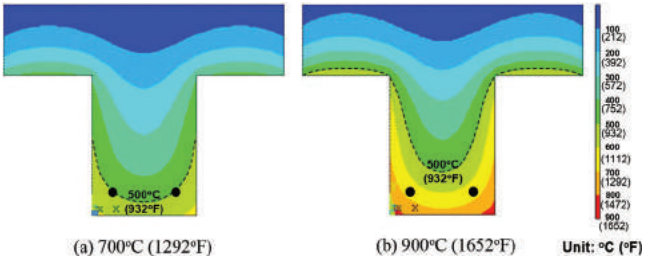

Fig. 12—Peak temperature distributions in beam section predicted by 2-D FEM.

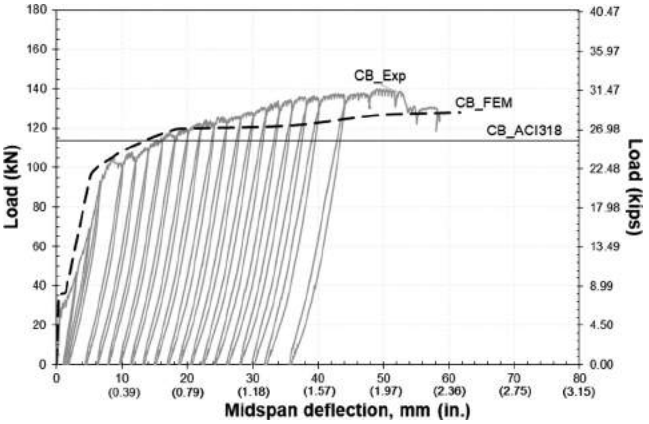

Fig. 13—Measured versus predicted load-deflection relationship of Beam CB.

of RC beams subjected to the sustained loading at elevated temperatures increased once the steel temperature exceeded 500°C (932°F). However, none of the beams failed before 3 hours based on the deflection criterion.

3. The effect of sustained loading at elevated temperatures on the post-fire flexural response of RC beams was significant at both 700 and 900°C (1292 and 1652°F) exposures. It decreased the stiffness, strength, and ductility of fire-damaged RC beams. The effect was more pronounced on the post-fire stiffness and ductility than strength.

4. Due to the presence of pre-existing cracks caused by heating and cooling (fire damage), all fire-damaged beams showed no cracking load.

5. A simplified 2-D FE transient thermal analysis can be used to predict the temperature response and fire resistance time of fire-exposed RC beams. Then, a simplified 3-D FE nonlinear structural analysis or an ACI approach could be adopted for a practical evaluation of post-fire flexural strength of RC beams subjected to low sustained service loads during fire exposure.

AUTHOR BIOS

Chanachai Thongchom *is a PhD Candidate in the Department of Civil Engineering at Chulalongkorn University, Bangkok, Thailand. He received his BS from Thammasat University, Pathumthani, Thailand. His research interests include fire-damaged reinforced concrete (RC) structures, fiber-reinforced polymer (FRP) strengthening, and repair of structures.*

Akhrawat Lenwari *is an Associate Professor of civil engineering at Chulalongkorn University. His research interests include strengthening and repair of bridges and buildings, fatigue and fracture mechanics, finite element analysis, composite structures, and FRP materials.*

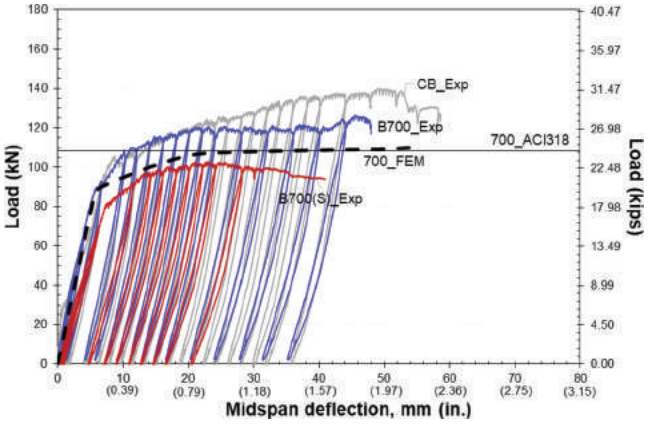

Fig. 14—Measured versus predicted load-deflection relationships of Beams B700 and B700(S).

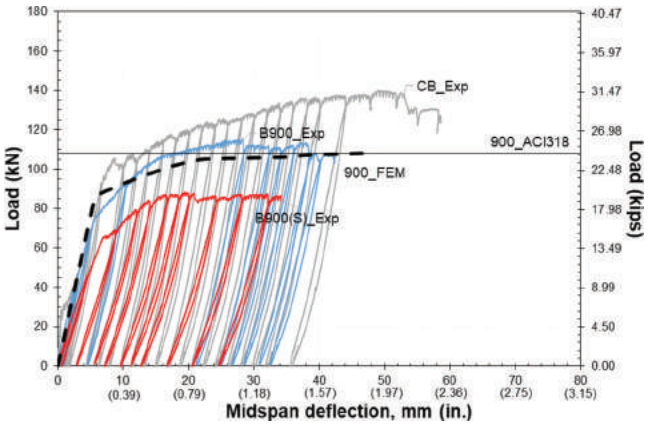

Fig. 15—Measured versus predicted load-deflection relationships of Beams B900 and B900(S).

Riyad S. Aboutaha, *FACI, is an Associate Professor of civil engineering at Syracuse University, Syracuse, NY. His research interests include structural evaluation of deteriorated concrete structures, sustainable concrete construction, and strengthening of RC structures.*

ACKNOWLEDGMENTS

The research was supported by the Thailand Research Fund (TRF) and Chulalongkorn University under the TRF Research Career Development Grant (Grant No. RSA6080019). The first author would like to acknowledge the financial support from the TRF through the Royal Golden Jubilee Ph.D. Program (Grant No. PHD/0135/2556).

NOTATION

A_s, A_s', A_s''	=	areas of steel reinforcements near web bottom, flange bottom, and flange top, respectively
b_f, b_w	=	web thickness and flange width, respectively
c	=	neutral axis depth
d, d', d''	=	distances from extreme compression fiber to steel reinforcements near web bottom, flange bottom, and flange top, respectively
E_c	=	elastic modulus of concrete
E_{pT}	=	residual elastic modulus at onset of strain hardening
E_s', E_s''	=	elastic modulus of steel reinforcements near flange bottom and flange top, respectively
E_{sT}	=	residual elastic modulus of steel reinforcement
f_c'	=	maximum compressive stress
f_r	=	modulus of rupture of concrete
f_{sT}	=	stress of steel reinforcement
f_{uT}	=	residual tensile strength of steel reinforcement
f_y', f_y''	=	yield strength of steel reinforcements near flange bottom and top, respectively
f_{yT}	=	residual yield strength of steel reinforcement

F_c, F_{sT}, F_s', F_s'' = internal forces in concrete and steel reinforcements near web bottom, flange bottom, and flange top, respectively
L = span length of beam
M_n = nominal post-fire flexural strength
p = strain hardening exponent
t_f = flange thickness
β_1 = factor relating depth of equivalent rectangular compressive stress block to neutral axis depth
ε_o = strain of concrete corresponding to maximum compressive stress
ε_{pT} = residual strain at onset of strain hardening
ε_s = strain of steel reinforcement
ε_{uT} = residual ultimate strain corresponding to ultimate strength
ε_y', ε_y'' = yield strain of steel reinforcements near flange bottom and top, respectively
ε_{yT} = residual yield strain of steel reinforcement

REFERENCES

1. Ellingwood, B., and Lin, T. D., "Flexure and Shear Behavior of Concrete Beams during Fires," *Journal of Structural Engineering*, ASCE, V. 117, No. 2, 1991, pp. 440-458. doi: 10.1061/(ASCE)0733-9445(1991)117:2(440)

2. Naus, D. J., "The Effect of Elevated Temperature on Concrete Materials and Structures—A Literature Review," *Report* No. ORNL/TM-2005/553, Oak Ridge National Laboratory, Oak Ridge, TN, 2005.

3. SFPE, *SFPE Handbook of Fire Protection Engineering*, fifth edition, Society of Fire Protection Engineers, Springer, New York, 2016.

4. Anderberg, Y., and Thelandersson S., "Stress and Deformation Characteristics of Concrete at High Temperatures," Lund Institute of Technology, Lund, Sweden, 1976.

5. Bratina, S.; Saje, M.; and Planinc, I., "The Effects of Different Strain Contributions on the Response of RC Beams in Fire," *Engineering Structures*, V. 29, No. 3, 2007, pp. 418-430. doi: 10.1016/j.engstruct.2006.05.008

6. Khalaf, J.; Huang, Z.; and Fan, M., "Analysis of Bond-Slip between Concrete and Steel Bar in Fire," *Computers & Structures*, V. 162, 2016, pp. 1-15. doi: 10.1016/j.compstruc.2015.09.011

7. Dwaikat, M. B., and Kodur, V. K. R., "Response of Restrained Concrete Beams under Design Fire Exposure," *Journal of Structural Engineering*, ASCE, V. 135, No. 11, 2009, pp. 1408-1417. doi: 10.1061/(ASCE)ST.1943-541X.0000058

8. Neves, I.; Rodrigues, J. P. C.; and Loureiro, A. D. P., "Mechanical Properties of Reinforcing and Prestressing Steels after Heating," *Journal of Materials in Civil Engineering*, ASCE, V. 8, No. 4, 1996, pp. 189-194. doi: 10.1061/(ASCE)0899-1561(1996)8:4(189)

9. Felicetti, R.; Gambarova, P. G.; and Meda, A., "Residual Behavior of Steel Rebars and R/C Sections after a Fire," *Construction and Building Materials*, V. 23, No. 12, 2009, pp. 3546-3555. doi: 10.1016/j.conbuildmat.2009.06.050

10. Lenwari, A.; Rungamornrat, J.; and Woonprasert, S., "Axial Compression Behavior of Fire-Damaged Concrete Cylinders Confined with CFRP Sheets," *Journal of Composites for Construction*, ASCE, V. 20, No. 5, 2016, pp. 296-303. doi: 10.1061/(ASCE)CC.1943-5614.0000683

11. El-Hawary, M. M.; Ragab, A. M.; El-Azim, A. A.; and Elibiari, S., "Effect of Fire on Flexural Behaviour of RC Beams," *Construction and Building Materials*, V. 10, No. 2, 1996, pp. 147-150. doi: 10.1016/0950-0618(95)00041-0

12. Hansanti, S., "Behaviors of Reinforced Concrete Beams after Fire," master's thesis, Chulalongkorn University, Bangkok, Thailand, 2001. (in Thai)

13. Kumar, A., and Kumar, V., "Behaviour of RCC Beams after Exposure to Elevated Temperatures," *Journal of the Institution of Engineers (India)*, V. 84, No. 3, 2003, pp. 165-170.

14. Xu, Y. Y.; Wu, B.; Jiang, M.; and Huang, X., "Experimental Study on Residual Flexural Behavior of Reinforced Concrete Beams after Exposure to Fire," *Advanced Materials Research*, V. 457-458, 2012, pp. 183-187. doi: 10.4028/www.scientific.net/AMR.457-458.183

15. Lakhani, H.; Singh, T.; Sharma, A.; Reddy, G. R.; and Singh, R. K., "Prediction of Post Fire Load Deflection Response of RC Flexural Members Using Simplistic Numerical Approach," *Structural Engineering and Mechanics*, V. 50, No. 6, 2014, pp. 755-772. doi: 10.12989/sem.2014.50.6.755

16. Ožbolt, J.; Bošnjak, J.; Periškić, G.; and Sharma, A., "3D Numerical Analysis of Reinforced Concrete Beams Exposed to Elevated Temperature," *Engineering Structures*, V. 58, 2014, pp. 166-174. doi: 10.1016/j.engstruct.2012.11.030

17. Kodur, V. K., and Agrawal, A., "Critical Factors Governing the Residual Response of Reinforced Concrete Beams Exposed to Fire," *Fire Technology*, V. 52, No. 4, 2016, pp. 967-993. doi: 10.1007/s10694-015-0527-5

18. Kodur, V. K. R., and Agrawal, A., "An Approach for Evaluating Residual Capacity of Reinforced Concrete Beams Exposed to Fire," *Engineering Structures*, V. 110, 2016, pp. 293-306. doi: 10.1016/j.engstruct.2015.11.047

19. ICC, "International Building Code," International Code Council, Falls Church, VA, 2015.

20. ISO 834-1, "Fire Resistance Tests—Elements of Building Construction. Part 1: General Requirement," International Standards Organization, Geneva, Switzerland, 1999.

21. ASTM E119-08a, "Standard Test Methods for Fire Tests of Building Construction and Materials," ASTM International, West Conshohocken, PA, 2008, 31 pp.

22. BS 476-20, "Fire Tests on Building Materials and Structures – Part 20: Method for Determination of the Fire Resistance of Elements of Construction (General Principles)," British Standards Institute, London, UK, 1987.

23. Willam, K.; Xi, Y.; Lee, K.; and Kim, B., "Thermal Response of Reinforced Concrete Structures in Nuclear Power Plants," SESM No. 02-2009, University of Colorado at Boulder, Boulder, CO, 2009.

24. Kodur, V. K. R., and Dwaikat, M. M. S., "Effect of High Temperature Creep on the Fire Response of Restrained Steel Beams," *Materials and Structures*, V. 43, No. 10, 2010, pp. 1327-1341. doi: 10.1617/s11527-010-9583-y

25. ANSYS, "ANSYS User's Manual," ANSYS, Inc., Canonsburg, PA, 2014.

26. Tiantongnukul, S., and Lenwari, A., "Thermal Analysis for Peak Temperature Distribution in Reinforced Concrete Beams after Exposure to ASTM E119 Standard Fire," *Engineering Journal (New York)*, V. 21, No. 4, 2017, pp. 243-258.

27. Lie, T. T., and Erwin, R. J., "Method to Calculate the Fire Resistance of Reinforced Concrete Columns with Rectangular Cross Section," *ACI Structural Journal*, V. 90, No. 1, Jan.-Feb. 1993, pp. 52-60.

28. Eurocode 2, "EN 1992-1-2: Design of Concrete Structures, Part 1-2: General Rules—Structural Fire Design," European Committee for Standardization, Brussels, Belgium, 2004.

29. Gao, W. Y.; Dai, J. G.; Teng, J. G.; and Chen, G. M., "Finite Element Modeling of Reinforced Concrete Beams Exposed to Fire," *Engineering Structures*, V. 52, 2013, pp. 488-501. doi: 10.1016/j.engstruct.2013.03.017

30. Kodur, V. K. R., and Dwaikat, B., "A Numerical Model for Predicting the Fire Resistance of Reinforced Concrete Beams," *Cement and Concrete Composites*, V. 30, No. 5, 2008, pp. 431-443. doi: 10.1016/j.cemconcomp.2007.08.012

31. Kodur, V. K. R.; Dwaikat, M. B.; and Fike, R. S., "An Approach for Evaluating the Residual Strength of Fire-Exposed RC Beams," *Magazine of Concrete Research*, V. 62, No. 7, 2010, pp. 479-488. doi: 10.1680/macr.2010.62.7.479

32. Tao, Z.; Wang, X.; and Uy, B., "Stress-Strain Curves of Structural and Reinforcing Steels after Exposure to Elevated Temperatures," *Journal of Materials in Civil Engineering*, ASCE, V. 25, No. 9, 2013, pp. 1306-1316. doi: 10.1061/(ASCE)MT.1943-5533.0000676

33. ACI Committee 318, "Building Code Requirements for Structural Concrete (ACI 318-14) and Commentary (ACI 318R-14)," American Concrete Institute, Farmington Hills, MI, 2014, 519 pp.